Distribution of scleractinian corals and stylasterid hydrocorals across abiotic environmental gradients on three seamounts in the Anegada Passage (#27834)

First submission

Guidance from your Editor

Please submit by 14 Feb 2020 for the benefit of the authors (and your \$200 publishing discount).



Structure and Criteria

Please read the 'Structure and Criteria' page for general guidance.



Raw data check

Review the raw data. Download from the materials page.



Image check

Check that figures and images have not been inappropriately manipulated.

Privacy reminder: If uploading an annotated PDF, remove identifiable information to remain anonymous.

Files

Download and review all files from the <u>materials page</u>.

- 9 Figure file(s)
- 6 Table file(s)
- 1 Raw data file(s)

Structure and Criteria



Structure your review

The review form is divided into 5 sections. Please consider these when composing your review:

- 1. BASIC REPORTING
- 2. EXPERIMENTAL DESIGN
- 3. VALIDITY OF THE FINDINGS
- 4. General comments
- 5. Confidential notes to the editor
- Prou can also annotate this PDF and upload it as part of your review

When ready <u>submit online</u>.

Editorial Criteria

Use these criteria points to structure your review. The full detailed editorial criteria is on your guidance page.

BASIC REPORTING

- Clear, unambiguous, professional English language used throughout.
- Intro & background to show context.
 Literature well referenced & relevant.
- Structure conforms to <u>PeerJ standards</u>, discipline norm, or improved for clarity.
- Figures are relevant, high quality, well labelled & described.
- Raw data supplied (see <u>PeerJ policy</u>).

EXPERIMENTAL DESIGN

- Original primary research within Scope of the journal.
- Research question well defined, relevant & meaningful. It is stated how the research fills an identified knowledge gap.
- Rigorous investigation performed to a high technical & ethical standard.
- Methods described with sufficient detail & information to replicate.

VALIDITY OF THE FINDINGS

- Impact and novelty not assessed.
 Negative/inconclusive results accepted.
 Meaningful replication encouraged where rationale & benefit to literature is clearly stated.
- All underlying data have been provided; they are robust, statistically sound, & controlled.
- Speculation is welcome, but should be identified as such.
- Conclusions are well stated, linked to original research question & limited to supporting results.

Standout reviewing tips



The best reviewers use these techniques

Τ	p

Support criticisms with evidence from the text or from other sources

Give specific suggestions on how to improve the manuscript

Comment on language and grammar issues

Organize by importance of the issues, and number your points

Please provide constructive criticism, and avoid personal opinions

Comment on strengths (as well as weaknesses) of the manuscript

Example

Smith et al (J of Methodology, 2005, V3, pp 123) have shown that the analysis you use in Lines 241-250 is not the most appropriate for this situation. Please explain why you used this method.

Your introduction needs more detail. I suggest that you improve the description at lines 57-86 to provide more justification for your study (specifically, you should expand upon the knowledge gap being filled).

The English language should be improved to ensure that an international audience can clearly understand your text. Some examples where the language could be improved include lines 23, 77, 121, 128 - the current phrasing makes comprehension difficult.

- 1. Your most important issue
- 2. The next most important item
- 3. ...
- 4. The least important points

I thank you for providing the raw data, however your supplemental files need more descriptive metadata identifiers to be useful to future readers. Although your results are compelling, the data analysis should be improved in the following ways: AA, BB, CC

I commend the authors for their extensive data set, compiled over many years of detailed fieldwork. In addition, the manuscript is clearly written in professional, unambiguous language. If there is a weakness, it is in the statistical analysis (as I have noted above) which should be improved upon before Acceptance.



Distribution of scleractinian corals and stylasterid hydrocorals across abiotic environmental gradients on three seamounts in the Anegada Passage

Steven R Auscavitch $^{\text{Corresp., 1}}$, Jay J Lunden $^{\text{1}}$, Alexandria Barkman $^{\text{1}}$, Andrea M Quattrini $^{\text{2}}$, Amanda W J Demopoulos $^{\text{3}}$, Erik E Cordes $^{\text{1}}$

Corresponding Author: Steven R Auscavitch Email address: steven.auscavitch@temple.edu

The distribution and diversity patterns of scleractinian corals and stylasterid hydrocorals at sub-photic depths are poorly studied compared to their shallow water relatives. In this study, we examined the distribution and diversity of hard coral assemblages on three highprofile seamounts within the Anegada Passage, a deep-water throughway linking the Caribbean and western North Atlantic. Using remotely operated vehicle surveys we characterized hard coral assemblages and overlying environmental variables between 162-2157 m on Dog Seamount, Conrad Seamount, and Noroît Seamounts. In all, 13 morphospecies of scleractinian and stylasterid corals were identified from video with stylasterids being more abundant than both colonial and solitary scleractinians. Cosmopolitan framework-forming corals Madrepora oculata and Solenosmilia variabilis occurred in patchy distributions largely at or above the aragonite saturation horizon with stylasterid hydrocorals being the only coral taxon observed below Ω_{arag} values of 1. Coral assemblage variation was found to be strongly associated with depth and aragonite saturation state, while others including temperature exhibited less pronounced responses. This study enhances our understanding of the factors that govern scleractinian and stylasterid coral distribution in an underreported marginal sea and establishes a baseline for monitoring expected environmental changes due to ocean acidification and deoxygenation in the tropical western Atlantic.

¹ Department of Biology, Temple University, Philadelphia, PA, USA

² National Museum of Natural History, Smithsonian Institution, Washington, D.C., United States

³ Wetland and Aquatric Research Center, US Geological Survey, Gainesville, Florida, USA



1	This information is distributed solely for the purpose of pre-dissemination peer review and must
2	not be disclosed, released, or published until after approval by the U.S. Geological Survey
3	(USGS). It is deliberative and pre-decisional information and the findings and conclusions in the
4	document have not been formally approved for release by the USGS. It does not represent and
5	should not be construed to represent any USGS determination or policy.
6	
7 8 9 10	Distribution of scleractinian corals and stylasterid hydrocorals across abiotic environmental gradients on three seamounts in the Anegada Passage
11 12 13	Steven R. Auscavitch ¹ , Jay J. Lunden ¹ , Alexandria Barkman ¹ , Andrea M. Quattrini ² , Amanda W.J. Demopoulos ³ , Erik E. Cordes ¹
14 15 16 17	 Department of Biology, Temple University, Philadelphia, PA, USA. National Museum of Natural History, Smithsonian Institution, Washington, DC. USA. Wetland and Aquatic Research Center, US Geological Survey, Gainesville, FL, USA.
18 19 20 21 22	Corresponding Author: Steven R. Auscavitch ¹ 1900 N 12 th St. Philadelphia, PA, 19122, USA.
23 24	Abstract
25	The distribution and diversity patterns of scleractinian corals and stylasterid hydrocorals
26	at sub-photic depths are poorly studied compared to their shallow water relatives. In this study,
27	we examined the distribution and diversity of hard coral assemblages on three high-profile
28	seamounts within the Anegada Passage, a deep-water throughway linking the Caribbean and
29	western North Atlantic. Using remotely operated vehicle surveys we characterized hard coral
30	assemblages and overlying environmental variables between 162-2157 m on Dog Seamount,
31	Conrad Seamount and Noroît Seamounts. In all 13 morphospecies of scleractinian and



stylasterid corals were identified from video with stylasterids being more abundant than both colonial and solitary scleractinians. Cosmopolitan framework-forming corals $Madrepora\ oculata$ and $Solenosmilia\ variabilis\ occurred\ in\ patchy\ distributions\ largely\ at\ or\ above\ the\ aragonite\ saturation\ horizon\ with\ stylasterid\ hydrocorals\ being\ the\ only\ coral\ taxon\ observed\ below\ <math>\Omega_{arag}$ values of 1. Coral assemblage variation was found to be strongly associated with depth and aragonite saturation state, while others including temperature exhibited less pronounced responses. This study enhances our understanding of the factors that govern scleractinian and stylasterid coral distribution in an underreported marginal sea and establishes a baseline for monitoring expected environmental changes due to ocean acidification and deoxygenation in the tropical western Atlantic.

Introduction

Global and regional modelling efforts in parallel with observational studies have contributed to our understanding of the distribution of framework-forming azooxanthellate corals in the deep sea (>200 m depth). However, a significant number of data deficient localities persist, most often hindered by a lack of records from direct seafloor observation and *in situ* environmental data. A number of environmental variables have been observed to control the distribution of deep-water azooxanthellate scleractinian corals and stylasterid hydrocorals, including parameters linked to depth, terrain, hydrography, and seawater chemistry (Davies & Guinotte, 2011). In the tropical western Atlantic, a center for deep-water scleractinian diversity (Cairns, 2007), additional direct observational data is needed to validate modelling efforts.

The growth of a scleractinian coral colony and formation of the aragonitic calcium carbonate skeleton is generally dependent upon the ambient seawater aragonite saturation state



56

57

58

59

60

61

62

63

64

65

66

67

68

69

70

71

72

73

74

75

76

77

 (Ω_{arag}) being greater than 1, or supersaturated. However, some deep-water scleractinian corals, including the cosmopolitan species Solenosmilia variabilis and Enallopsammia rostrata, have been reported well below the saturation horizon (the depth at which $\Omega_{arag} = 1$) on Tasmanian seamounts (Thresher et al., 2011). A more recent survey of seamounts in the Northwestern Hawaiian Islands and Emperor Seamounts documented living colonial scleractinian reefs at Ω_{arag} as low as 0.71 (Baco et al., 2017). Previous studies lend support for targeted observational surveys in underexplored regions in order to delineate species distribution patterns with respect to aragonite saturation and other environmental variables. These efforts are particularly salient in light of potential and ongoing anthropogenic impacts to deep-sea coral ecosystems, including global climate change and ocean acidification, deep-water drilling and resource extraction, and bottom-contact fishing, and deep-sea crust mining. The Greater-Lesser Antilles transition zone is one of the most sparsely surveyed yet biogeographically important deep-water entries from the western Atlantic Ocean into the Caribbean Basin. Topographic features, such as seamounts and other submarine rises associated with tectonic plate boundaries, are important contributors to the environmental complexity of the deep-sea benthos. In the Anegada Passage, Dog Seamount, Conrad Seamount, and Noroît Seamount are the most prominent of several high-profile seamounts and banks present, covering abyssal to mesophotic depths. Typical environmental characteristics of seamounts, including substrate heterogeneity, enhanced productivity and carbon flux, and variable currents (Rogers, 2018), create the potential for deep-water biodiversity hotspots in this area and potential elevated species abundance relative to surrounding continental shelf and slope habitats. Previous studies indicate that at depths > 200 m, azooxanthellate corals generally prefer hard substrata that exhibit topographic complexity (Roberts et al., 2009; Georgian, Shedd & Cordes, 2014). As such,



79 hard substrate for corals (Rogers, 1994). Yet very few seamount faunal communities in the Caribbean have been characterized with respect to these important abiotic gradients. 80 81 Throughout the tropical western Atlantic, scleractinian species diversity and distributions 82 are relatively well-known from shallow waters but the extent of their distribution below 150 m is 83 poorly understood. For deep-water azooxanthellate corals, 81 species have been reported at depths greater than 50 m for the Greater and Lesser Antilles (Cairns, 2007). Efforts have also 84 been made to understand the biogeographic context of Caribbean ecoregions using deep-water 85 86 corals in order to support conservation strategies (Cairns & Chapman, 2001; Miloslavich et al., 2010; Hernández-Ávila, 2014). In the Caribbean Basin, patterns in deep-sea coral beta diversity 87 88 (e.g., species turnover) between ecoregions have been attributed to topography and 89 oceanography (Hernández-Ávila, 2014). Within the insular Caribbean, the Greater Antilles and Lesser Antilles regions are found to diverge into two ecoregions, one encompassing the Greater 90 91 Antilles islands and the other the Lesser Antilles Islands, at continental slope depths (200-92 2000m). At larger biogeographic scales and evolutionary time, deep-water currents or water 93 masses have been hypothesized as distribution pathways for constraining cosmopolitan habitat-94 forming corals like *Lophelia pertusa* in the western Atlantic (Arantes et al., 2009; Henry, 2011). While widespread seamount surveys from the Caribbean Basin remain rare, the effect of 95 96 environmental variables like temperature, dissolved oxygen, and water mass has been 97 demonstrated for demersal fishes on seamounts in the Anegada Passage (Quattrini et al., 2017). The present study focuses on describing patterns in the distribution of deep-water 98 99 scleractinians and stylasterid hydrocorals on three prominent seamounts in the northeast 100 Caribbean Sea. We test the hypothesis that coral species that produce aragonitic skeletons can

seamounts are one example of topographically complex deep-water features that provide ideal



survive and produce skeletal framework above the aragonite saturation horizon in this region of the Western Atlantic Ocean. As a suspected driver of deep-water coral community structure, we also examine the relationship between water mass structure and community similarity in the bathyal zone, hypothesizing that different water masses would have distinct coral assemblages. Furthermore, this study will aim to identify the individual oceanographic variables that most strongly influence the presence of hard corals and their contribution to changes in community similarity for this locality.

Materials & Methods

ROV Surveys

This study examined sites within the Anegada Passage in the northeastern corner of the Caribbean Sea (Fig. 1). Three seamounts of varying depths (near-base to summit) were surveyed in September 2014 using the ROV *Hercules* during E/V Nautilus cruise NA052 (Table 1). Three dives were conducted on Dog Seamount (276 to 1035 m depth), two were conducted on Conrad Seamount (162 to 1314 m depth), and two were conducted on Noroît Seamount (949 to 2206 m depth). Efforts were made to cover similar depth ranges on each feature for direct comparison as permitted by the bathymetry.

The ROV was deployed to a maximum target depth on each seamount and generally moved to shallower depths up slope. The ROV continuously traversed the seafloor as near to the bottom as practical at a slow, steady speed (~0.1-0.2 knots, ~0.1 m/s); however, transects were occasionally interrupted by stopping the ROV for sampling and detailed camera zooms. The ROV was equipped with a high-definition camera and paired scaling lasers (10 cm apart). During the dives, the forward-facing cameras were set on wide-angle view, but frequent snap-zooms (up



125 to 20 sec) were conducted to aid in species identification. The ROV was also equipped with a Seabird FastCAT 49 conductivity-temperature-depth (CTD) logger and an Aanderaa oxygen 126 127 optode to measure dissolved oxygen (DO). The ROV was tracked on the seafloor using an ultrashort baseline (USBL) tracking system as well as a Doppler Velocity Log (DVLNAV). 128 129 Seawater Collection and Carbonate Chemistry Analysis 130 Seawater samples (n = 34) were collected both in the water column and at the benthos 131 using Niskin bottles mounted to the ROV Hercules (Supplementary Table 1). On bottom, 132 seawater samples were collected within 1-2 meters of the benthos and usually co-occurred with 133 the observation of scleractinian colonies on the seafloor. For all seawater samples, co-located physical data (pressure, temperature, salinity, and oxygen) were obtained using vehicle mounted 134 135 conductivity-temperature-depth (Paroscientific Digiquartz, SBE 49Plus) and oxygen (Aanderaa 136 Optode 3830) sensors, respectively. Upon recovery of the ROV, samples were immediately transferred to 500 mL high-density polyethylene (HDPE) containers according to Best Practices 137 138 for Ocean CO₂ measurements (Dickson, Sabine & Christian, 2007). While HDPE containers are suitable for long-term storage of seawater for total alkalinity analyses (Huang, Wang & Cai, 139 140 2012), they are not suitable for long-term storage for pH or dissolved inorganic carbon analyses 141 as they are permeable to CO₂. Accordingly, pH was measured within 1 hour of collection 142 onboard the vessel. Immediately following pH measurement, samples were poisoned with 100 143 μL saturated mercuric chloride solution and stored in a cool, dark location. Total alkalinity was 144 measured in the laboratory in triplicate according to methods previously described (Lunden, Georgian & Cordes, 2013; Georgian et al., 2016a), and final Ω_{arag} values were computed using 145 146 CO2calc (Robbins et al., 2010). Due to the logistical challenge of pairing a discrete water sample 147 with each individual scleractinian coral observation, we generated a predictive model to





interpolate Ω_{arag} at the depth of each coral observation based on temperature, dissolved oxygen, and salinity (for methodology see (Georgian et al., 2016a).

150

151

152

153

154

155

156

157

158

159

160

161

162

163

164

165

166

167

148

149

ROV video analysis

Framework-forming coral colonies and individual solitary coral occurrences were documented using high-definition video transects during each of the ROV dives. Video segments where collections were made, where the vehicle was too high off bottom, moving backwards, or of generally poor quality, were removed from analysis. For the purposes of this analysis, framework-forming corals included members of the Scleractinia and hydrozoan family Stylasteridae. Stylasterids were included since they are reportedly diverse from this region, are functionally similar to framework-forming scleractinians in their ability to provide habitat to other species, and are composed of aragonitic coralla (Cairns, 2011). Consistent morphospecies (msp) identification were used throughout the analyses. Voucher specimens for morphological identification were obtained using the ROV platform. If necessary, further identification of coral species were made using taxonomic keys and assistance from taxonomic specialists. Colony height was measured, where possible, by referencing scaling lasers. Individuals or colonies were typically identifiable above a 5-cm height threshold based on laser scalers. If occurrences could not be readily identified below the 5-cm threshold, they were omitted from analysis. Each occurrence was paired with an associated time-stamp relating to in situ environmental metadata (temperature, depth, dissolved oxygen concentration, and salinity).

168169

Community Analyses

170171

172

In order to assess the community relationships among hard-coral assemblages, species abundance values were binned into 100 m depth segments for each seamount transect resulting in



28 total samples. First, sampling effort was evaluated for both seamounts individually and all
seamounts combined by sample-based species accumulation curves. Community-level analyses
were conducted using standardized and 4^{th} root transformed species abundance data in PRIMER
v7 with PERMANOVA add-on (Clarke & Gorley, 2006; Anderson, Gorley & Clarke, 2008).
Transformed and standardized species abundances were compiled into a Bray-Curtis
resemblance matrix for further analyses. In order to test for significant differences among hard
coral assemblages on different seamounts, a one-way analysis of similarity (ANOSIM) was
conducted between features as well as between local water masses. Non-metric multidimensional
scaling ordinations (nMDS) were conducted across all 28 samples. nMDS plots were overlaid
with similarity profile (SIMPROF) analysis to show significant groupings of samples at the 95%
level or greater (Clarke, Somerfield & Gorley, 2008). Similarity percentage (SIMPER) tests were
used to identify taxa that contributed disproportionately to assemblage similarities within and
between seamounts and water masses.
Multivariate analyses were also used to explore the abiotic variables relevant to the variation
observed in the distribution data. Environmental data for temperature, salinity, dissolved oxygen,
and Ω_{arag} were obtained from the calculated mean in each 100m depth segment within every
transect. The mean was then 4th-root transformed and normalized within each variable he
BEST (BIO-ENV) routine (Clarke, Somerfield & Gorley, 2008) was applied to the dataset to
which environmental variables would be useful predictor variable distance-based linear
model (DistLM) with Akaike information criterion (AIC) was applied using the PERMANOVA
add-on in PRIMER v7 (Anderson, Gorley & Clarke, 2008). Visualizations of the resemblance
matrix with predictor variables were observed using a dbRDA (distance-based redundancy
analysis) ordination with DistLM overlay.



1	96
1	97

Results

Survey Summaries

A total of 106 hours of bottom time were assessed across 7 dives (Table 1). Video records were annotated between the depth range of 162-2157 m. In all, 264 observations of solitary and framework-forming scleractinian corals and stylasterid hydrocorals were made across all three seamounts (Table 2). Three dives at Dog Seamount yielded 64 records from 284-849m. From Conrad Seamount, 182 records were made from 166m to 1230m across 2 dives. The deepest two dives at Noroît Seamount had 18 records reported from 1014-1626m. Stylasterids made up the majority (53%) of coral observations, however most were observed at depths shallower than 400m (Table 2). The majority of scleractinians observed were colonial, framework-forming species (100 colonies observed) while only 22 observations were made of solitary coral species. No scleractinians or stylasterids were deeper than 1626m on any seamount.

Water Mass Analysis

Downcast CTD profiles from the ROV sensors were plotted and assessed at each seamount using Ocean Data View v4 (Fig. 2) Multiple dive profiles for each seamount were combined to create one consensus profile for that locality. Water masses were identified following published records based on temperature, salinity, and dissolved oxygen profiles for the northeast Caribbean and Anegada Passage (Morrison & Nowlin, 1982). Major water masses in the northeast Caribbean that were identified here include Subtropical Underwater (SUW), Sargasso Sea Water



PeerJ

221	(SSW), Tropical Atlantic Central Water (TACW), Antarctic Intermediate Water (AAIW), and
222	North Atlantic Deep Water (NADW) (>1200m) (Quattrini et al., 2017).
223	
224	Carbonate chemistry analysis
225	Water samples for carbonate chemistry analyses were collected at depth from 50 m to
226	2170 m. Total alkalinity ranged from 2291.4 to 2405.9 μ mol·kg ⁻¹ , and pH ranged from 7.83 to
227	8.11, with minimum pH observed at 795 m depth. Measured Ω_{arag} values from Niskin bottle
228	collections ranged from 4.13 at 50 m depth to 0.99 at 2170 m depth. The aragonite saturation
229	state of the water column was reliably predictable according to the following equation: $\Omega_{arag} = (T_{arag})^T + (T_{arag})$
230	\times 0.11407018) + (O \times 0.00302922) + (S \times 0.18168448) – 6.5216044 (stepwise backward
231	regression, $R^2 = 0.9857$, p < 0.001) where $T =$ temperature in °C, $O =$ oxygen concentration in
232	μ mol·L ⁻¹ , and S = salinity in parts per thousand (ppt). From this, predicted Ω_{arag} values ranged
233	from 4.11 to 1.05, with highest value at 51 m at Dog Seamount and lowest value at 2195 m at
234	Noroît Seamount.
235	
236	Coral species Distribution Patterns
237	The most abundant scleractinian coral was <i>Solenosmilia variabilis</i> (44 colonies) but it

The most abundant scleractinian coral was *Solenosmilia variabilis* (44 colonies), but it was only observed on Conrad Seamount in a relatively narrow depth range, 409-569 m. Many colonies were found to be associated with boulder and low, outcropping, hard-rock substrate. This was followed by the more widespread *Madrepora oculata* (22 colonies), which occurred between 784 and 1540 m on all seamounts (Fig. 3). *Madrepora oculata*, which displayed at least 2 different growth forms from thin and twiggy branches to thick, robust colonies, possessed the widest depth distribution range for any colonial scleractinian coral. The deepest solitary



scleractinian coral, *Javania cailleti*, was observed at 1626m; this occurrence corresponds with one of the lowest measured Ω_{arag} values of 1.01.

The upper bathyal depths shallower than 700m presented species with narrower depth distributions compared to lower bathyal depths (>800m) (Fig. 3). The sub-700m assemblage was composed of three species of scleractinians (*Enallopsammia rostrata*, *M. oculata*, and *J. cailleti*) and one stylasterid (*Crypthelia* sp. 1). The shallowest depths, usually coinciding with the seamount summit, were dominated by two species of stylasterids, *Stylaster* sp. 1 and *Stylaster* cf. *duchassaingi*, as well as one azooxanthellate scleractinian, *Madracis myriaster* (Milne Edwards & Haime, 1849). On Conrad Seamount, pink and purple coralline algal crusts were observed as deep as 256m depth and continued to be observed through shallower depths dominated by sponges, stylasterids, and black corals.

The majority of stylasterid species were restricted to depths <400m with the only taxon exhibiting a wider depth distribution was the genus *Crypthelia* (Fig. 3). Only 3 morphospecies of stylasterids were large enough to be consistently identified during video annotation. Other unidentifiable stylasterids were lumped into a fourth group, unidentified Stylasteridae. The most abundant species, *Stylaster* sp. 1, was found in a narrow depth range between 166-174m on the summit of Conrad Seamount.

Patterns of Coral Occurrences with Aragonite Saturation State

Measured Ω_{arag} values from water collected adjacent to corals varied compared to what was predicted using the predictive aragonite saturation state model data. Based on measured values from the water samples collected adjacent to the coral observations, all observations occurred at or above the aragonite saturation horizon ($\Omega_{arag} > 1$) (Table 3). Multiple water





samples were collected for only *Madrepora oculata*. A full table of all 34 Niskin water bottle measurements and matched environmental variables is provided (Supplementary Table 1).

Using predicted values derived from CTD and sensor data on temperature, oxygen concentration, and salinity, all scleractinian and stylasterid corals were observed at Ω_{arag} values of 0.99 to 3.45 (Fig. 4). For scleractinians, *Javania cailleti* occurred across the largest aragonite saturation state range, between 1.01 and 1.77. Among the Stylasteridae, *Crypthelia* sp. 1 occurred across the greatest range of saturation states from as low as 0.99 up to 2.83. Only three species were observed at or around the aragonite saturation horizon based on predicted saturation state values, Crypthelia sp. 1 ($\Omega_{arag} = 0.99$), *M. oculata* ($\Omega_{arag} = 1.00$) and *J. cailleti* ($\Omega_{arag} = 1.01$).

Community Structure Patterns

Species-accumulation curves were evaluated for seamounts individually and in aggregate for all seamounts. Combined, all seamounts (100-1700m) revealed a more complete sampling effort than among single seamount coral assemblages (Fig. 5). Individually, species accumulation curves for Dog, Conrad, and Noroît Seamount were not asymptotic, and therefore are likely to accumulate additional coral morphospecies with increased sampling effort.

Analysis of similarity (two-way nested, depth within seamount, Global R=0.122, p=0.05) conducted between seamount revealed significant differences in coral assemblages between Dog and Noroît Seamounts (R=0.544, p=0), but not Conrad and Dog Seamounts (R=-0.001, p=0.38) or Conrad and Noroît Seamounts (R=0.029, p=0.001) (Supplementary Table 2). A one-way ANOSIM (Global R=0.464, p=0.001) between water masses revealed significant differences in assemblages between SSW and TACW (R=0.46, p=0.004), AAIW (R=0.53, p=0.002), and



289 NADW (R=0.60, p=0.008) as well as between TACW and NADW (R=0.93, p=0.001) and 290 AAIW and NADW (R=0.361, p=0.01) (Supplementary Table 3). 291 Non-metric multi-dimensional ordination with SIMPROF groupings revealed five statistically significant groupings; two shallow assemblages composed of samples from between 100-600 m 292 293 and 200-400m, two mid-depth assemblages (500-700m and 700-1100 m), and one deep 294 assemblage (1100-1600m) (Fig. 6). Outliers from these groupings occurred at 600-700 m and 295 1100-1200 m on Conrad seamount and between 1300-1400 m on Noroît Seamount. Within 296 SIMPROF groupings, the shallowest depth grouping showed the greatest amount of dissimilarity 297 among samples (a metric of beta diversity) among the three while the lowest occurred in the 298 deepest group. 299 Dog Seamount exhibited the lowest beta diversity among all three seamounts and highest 300 average similarity at 61% (one-way SIMPER analysis), with the average similarity between 301 samples being most strongly influenced by *Crypthelia* sp. 1, which contributed to 96.6% of the 302 relative abundance. Noroît Seamount had the second highest similarity (38.2%), with *Madrepora* oculata accounting for 84.7% of the similarity. Conrad Seamount had the lowest average 303 304 similarity (15%), with stylasterids Crypthelia sp. 1 and Stylaster cf. duchassaingi being the 305 greatest contributors to average similarity with 48.4% and 21.5%, respectively. Between 306 seamounts, Noroît differed from Dog and Conrad, primarily due to the higher abundance of 307 Madrepora oculata at Noroît Seamount. Noroît Seamount had nearly triple the average 308 abundance of Madrepora oculata compared to Conrad Seamount. Conrad and Dog Seamounts 309 differed primarily due to the contribution of Crypthelia sp. 1 and Madracis myriaster, which 310 were present on Conrad at 2 to 3 times higher average abundance at Dog Seamount.





whilin water masses, the greatest average similarity occurred within NADW (34%) followed
by TACW (51%) and finally SSW at (32 %). The abundance of scleractinians were responsible
for greater similarities within deep water masses (Madrepora oculata and Javania cailleti in
NADW) while stylasterids were more commonly associated with driving patterns of similarity
within intermediate and shallower water masses (Crypthelia sp. 1 in TACW, AAIW and
Stylaster cf. duchassaingi in SSW). Between immediately adjacent water masses, the greatest
average dissimilarity was observed between SUW and SSW (92.3%) and the lowest between
TACW and AAIW (56.7%), indicating the highest rates of turnover (beta diversity) between
shallower water masses than deeper ones.
Results from the BEST analysis indicated that the largest percentage of biological variation
was correlated with depth (r=0.536). The BEST routine also indicated that the greatest
correlation occurred with the four combined factors of depth, Ω_{arag} , temperature, and dissolved
oxygen (r=0.614). Sequential tests in the distLM analysis indicated that depth (AIC=223.88,
p=0.001) and Ω_{arag} (AIC= 215.87, p=0.001) were the greatest explanatory variables influencing
coral assemblages on seamounts in the Anegada Passage. Temperature, salinity, and oxygen did
not explain a significant portion of the biological variation in sequential testing. Redundancy
analyses resulted in 59.4% of the DistLM model variation explained by the primary axis
(dbrda1) and 32.6% explained by the second (dbrda2) (Fig. 7). Likewise, the first axis explained
32.8% of the total biological variation observed followed by 18% explained by the second axis.
The primary axis was most closely correlated with oxygen ($r = -0.82$), while the second was most
closely related to temperature (r= -0.61).



Discussion

Seamounts in the Anegada Passage were found to harbor communities of stony and lace
throughout the bathyal depth range from summit depths as shallow as 166 m to a maximum of
1626 m. We found that both stylasterid and scleractinian coral species with aragonitic skeletons
were largely present above the aragonite saturation horizon in this region of the Western Atlantic
Ocean Only stylasterids in the genus <i>Crypthelia</i> were observed to occur below the aragonite
saturation horizon ($\Omega_{arag} = 0.99$), but others, including the framework forming species <i>Madrepora</i>
oculata, occurred at saturations states as low as $\Omega_{arag} = 1.0$. Overlying water masses were a
significant indicator of community assembly differences between SSW (Sargasso Sea Water)
and deeper water masses, but not between the shallowest water mass, Subtroptical Underwater
(SUW). Oceanographic variables that most strongly influenced the presence of aragonitic corals
and their contribution to changes in community similarity were depth and aragonite saturation
state, with temperature, salinity, and dissolved oxygen making less significant contributions.
The tropical western Atlantic is a known diversity center for azooxanthellate scleractinian
corals and stylasterid hydrocorals (Cairns, 2007, 2011). This study provides new distribution
records and voucher specimens for several cosmopolitan scleractinian coral species in the
northeastern Caribbean. Prior to this expedition, azooxanthellate coral distributions were poorly
known in deep waters of the eastern Caribban. In addition, 7 species or morphospecies of stony
corals within the genera Javania, Madrepora, Madracis, Enallopsammia, Dendrophyllia, and
Caryophyllia have been added to local species inventories in the Anegada Passage (Fig. 8). New
records from photographic and physical specimens aid in resolving the complex biogeography of
the Greater-Lesser Antilles Transition zone seamounts with respect to the western North
Atlantic. The paucity of records paired with environmental parameters from global





358

359

360

361

362

363

364

365

366

367

368

369

370

371

372

373

374

375

376

377

378

biogeographic databases makes these observations critical to understanding the species distribution dynamics of marginal Atlantic seas and how coral distribution may be affected by future ocean climatic changes.

Stony coral assemblages in the northeast Caribbean are similar to those observed in other parts of the western Atlantic Ocean with a few noteworthy absences. Absent from our records from the Anegada Passage seamounts include Lophelia pertusa, Enallopsammia profunda, and cosmopolitan cup coral species like *Desmophyllum dianthus*, which are more common throughout the US southeast continental shelf and Gulf of Mexico (Schroeder et al., 2005; Reed, Weaver & Pomponi, 2006; Brooke & Schroeder, 2007). While fossilized Lophelia rubble has been reported in the Colombian Caribbean (Santodomingo et al., 2007) and ive Lophelia has been observed on the Brazilian continental margin (Arantes et al., 2009) and off Roatan, Honduras (Henry, 2011), it has not been extensively reported in the insular Caribbean (OBIS, 2019). Within the Greater and Lesser Antilles, communities at continental shelf depths have been found to be dissimilar enough from the southern Caribbean that they may constitute distinct ecoregions (Hernández-Ávila, 2014). These differences are primarily driven by the difference in the abundance of *Madracis* myriaster, which is common at mesophotic and upper bathyal depths, but becomes less common with increasing dept lowever, since many parts of the Caribbean remain poorly sampled (Miloslavich et al., 2010), a more rigorous nalysis incorporating more modern datasets would be required to elucidate biogeographic patterns across the basin. It is important to mention that a greater diversity of solitary scleractinian corals and smaller stylasterids was likely present in the video but could not be reported due to video resolution limitations. The lack of easily identifiable diagnostic features, small sizes, and low densities of



cup corals make most species difficult to identify from ROV surveys without detailed camera zooms or voucher specimens.

We also were able to determine local distribution patterns among seamounts and on a single seamount for several species. *Enallopsammia rostrata*, *Dendrophyllia alternata*, and *Solenosmilia variabilis* appear to have patchy distributions on the Anegada Passage seamounts. For example, *Enallopsammia rostrata* (2 colonies, Dog Seamount only) and *Dendrophyllia alternata* (5 colonies, Conrad Seamount only) were very rarely observed and only within narrow depth ranges, at 785 m and between 490-598 m, respectively. Likewise, *S. variabilis* was only observed in patches on Conrad Seamount from 490-569m. *Solenosmilia* has not been widely reported from the Greater Caribbean Basin, based on records from the Ocean Biogeographic Information System (OBIS, 2019). In the southern hemisphere, *Solenosmilia* has been more commonly reported to asexually reproduce, and thus has a relatively short dispersal ability (Miller & Gunasekera, 2017), potentially explaining its patchy distribution.

The ecological contribution of stylasterid corals is often understated, despite the ability of some species to produce significant structures that can act as habitat for associated invertebrate species. Large framework-forming stylasterids are functionally similar to reef-forming scleractinian corals in that they can provide habitat for larger organisms such as deep-water fishes and associated invertebrates (Häussermann & Försterra, 2007). *Crypthelia* spp., while relatively abundant in places and occurring over a wide range, were never observed above 12cm in overall height and were extremely brittle (Fig. 9A). However, two species in the genus *Stylaster*, *Stylaster* cf. *duchassaingi* (Fig. 9B) and *Stylaster* sp. 1 (Fig. 9C), can be classified as significant three-dimensional structure-forming species, primarily occurring between 150- 400 m depth. The carbonate mineralogy of most stylasterids is similar to scleractinians in that a



403

404

405

406

407

408

409

410

411

412

413

414

415

416

417

418

419

420

421

422

423

424

majority of known species, including those observed in this study, produce a skeleton composed primarily of the mineral aragonite (Cairns, 2011), although some are calcitic in composition (Cairns & Macintyre, 1992). Stylasterids do share distribution characteristics and overlapping depth ranges with many upper bathyal solitary and colonial scleractinian corals (Cairns, 1986, 2011). Also, like scleractinians, stylasterid hydrocorals also exhibit a vulnerability to changing aragonite saturation conditions over their depth distribution (Guinotte et al., 2006). Several species in the genus *Crypthelia* occur in the eastern Caribbean at bathyal depths (Cairns, 1986). The difficulty of identifying stylasterids from ROV video remains a challenge in establishing species occurrences, necessitating a voucher collection to confirm morphospecies identity. Nevertheless, the depth distribution, colony morphology, and coloration of *Stylaster* sp. 1, is consistent with Stylaster roseus (Pallas, 1766), a tropically-distributed western Atlantic stylasterid from depths typically <500m (OBIS, 2019). Crypthelia sp. and other stylasterids are more likely to be underreported due to their small size (2-5 cm), on the threshold of being able to be accurately recorded from ROV video. These stylasterids were also observed under overhangs which made obtaining an accurate account of their abundance difficult. In this case, the reported occurrences of these corals represent a minimum value. Knowledge of the chemical environment of deep-sea scleractinians has grown significantly in recent years as empirical measurements of the carbonate system at deep-sea coral habitats have been reported from different regions across the global ocean. On seamounts in the Indian Ocean off the coast of SW Australia, the majority of framework-forming scleractinians – including Enallopsammia rostrata and Solenosmilia variabilis – were found at Ω_{arag} values at or just below saturation, suggesting a control on the lower limit of these species' distributions

(Thresher et al., 2011). However, live scleractinian reefs were recently discovered on seamounts



in the North Pacific at Ω_{arag} values as low as 0.71 (Baco et al., 2017) and as low as 0.81 off Southern California (Gómez et al., 2018). These revelations indicate that, under the right conditions, scleractinian corals can persist in undersaturated waters (Baco et al., 2017). Additionally, the presence of live tissue may buffer against the effects of low pH (Venn et al., 2011), but the underlying dead coral framework may be less resilient to undersaturated waters. Productivity of the surface waters and export to the deep-sea benthos may be attributed to

differences in species distribution and abundance. In a 2016 laboratory experiment and field study comparing two spatially distinct and genetically isolated populations of the framework-forming scleractinian *Lophelia pertusa*, colonies from Norway exhibited enhanced respiration and prey capture rates under acidified conditions compared to individuals from the Gulf of Mexico (Georgian et al., 2016b). This study lends support to the hypothesis that species are locally adapted to environmental conditions, including food supply, which may allow individuals to better tolerate reduced carbonate saturation states. Furthermore, these findings lend support for targeted observational surveys in underexplored regions in order to delineate species distribution patterns with respect to environmental variables.

Conclusions

Our results offer some insights to the distribution, diversity, and drivers of community assembly of scleractinian and stylasterid deep-water corals in a data-deficient region of the tropical western Atlantic Ocean. The presence of aragonitic corals, largely occurring above the aragonite saturation horizon, was not unexpected, but more surprising was the presence of known reef-forming scleractinians, like *Madrepora oculata*, living at or just above $\Omega_{arag} = 1$. Future work should seek to expand upon coral communities beyond scleractinian and stylasterid corals, particularly to refine the relationship between community assembly and water mass



450

451

452

453

454

455

456

457

458 459

460

461

462

463

464

465

466 467

468

469

470

471

472

473

structure. Increased taxonomic effort is needed to better identify cryptic coral morphospecies in the deep-sea benthos. In the Atlantic Ocean, deep-water coral ecosystem health is likely to be negatively impacted by environmental change the end of the current century. Warming deepwaters (Gleckler et al., 2016), thermohaline driven deep-water acidification (Pérez et al., 2018), and low latitude deoxygenation in the Atlantic (Montes et al., 2016) are among the greatest threats facing deep-water framework-forming corals. The occurrence records and relationships between coral distribution and environmental variables reported here form a critical baseline for the detection of the effects of deep ocean change, which is crucial to effective conservation. **Acknowledgements** We would like to thank the efforts of the science party and crew of the E/V Nautilus on NA052: Exploration of the Anegada Passage. Taxonomic assistance in identifying some voucher material was provided by S. Cairns (NMNH) for scleractinian and stylasterid corals. Any use of trade, firm, or product names is for descriptive purposes only and does not imply endorsement by the U.S. Government. References Anderson M. Gorley RN, Clarke RK. 2008. Permanova+ for Primer: Guide to Software and Statisticl Methods. Primer-E Limited. Arantes RCM, Castro CB, Pires DO, Seoane JCS. 2009. Depth and water mass zonation and species associations of cold-water octocoral and stony coral communities in the southwestern Atlantic. Marine Ecology Progress Series 397:71–79. DOI: 10.3354/meps08230.



1/4	Baco AR, Morgan N, Roark EB, Silva M, Shamberger KEF, Miller K. 2017. Defying
175	Dissolution: Discovery of Deep-Sea Scleractinian Coral Reefs in the North Pacific.
176	Scientific Reports 7:1–11. DOI: 10.1038/s41598-017-05492-w.
77	Brooke S, Schroeder WW. 2007. State of deep coral ecosystems in the Gulf of Mexico region:
178	Texas to the Florida Straits. The State of Deep Coral Ecosystems of the United States:271-
179	306.
180	Cairns SD. 1986. A revision of the Northwest Atlantic Stylasteridae (Coelenterata: Hydrozoa).
181	Smithsonian Contributions to Zoology. DOI: 10.5479/si.00810282.418.
182	Cairns SD. 2007. Deep-water corals: An overview with special reference to diversity and
183	distribution of deep-water scleractinian corals. In: Bulletin of Marine Science.
184	Cairns SD. 2011. Global diversity of the stylasteridae (Cnidaria: Hydrozoa: Athecatae). <i>PLoS</i>
185	ONE 6. DOI: 10.1371/journal.pone.0021670.
186	Cairns SD, Chapman RE. 2001. Biogeographic affinities of the North Atlantic deep-water
187	Scleractinia.
88	Cairns SD, Macintyre IG. 1992. Phylogenetic implications of calcium carbonate mineralogy in
189	the Stylasteridae (Cnidaria: Hydrozoa). <i>Palaios</i> :96–107.
190	Clarke KR, Gorley RN. 2006. User manual/tutorial. PRIMER-E Ltd., Plymouth.
191	Clarke KR, Somerfield PJ, Gorley RN. 2008. Testing of null hypotheses in exploratory
192	community analyses: similarity profiles and biota-environment linkage. Journal of
193	Experimental Marine Biology and Ecology 366:56–69. DOI: 10.1016/j.jembe.2008.07.009
194	Davies AJ, Guinotte JM. 2011. Global habitat suitability for framework-forming cold-water
95	corals. PloS one 6:e18483.
96	Dickson AG, Sabine CL, Christian JR. 2007. Guide to best practices for ocean CO2



497	measurements. North Pacific Marine Science Organization.
498	Georgian SE, DeLeo D, Durkin A, Gomez CE, Kurman M, Lunden JJ, Cordes EE. 2016a.
499	Oceanographic patterns and carbonate chemistry in the vicinity of cold-water coral reefs in
500	the Gulf of Mexico: Implications for resilience in a changing ocean. Limnology and
501	Oceanography 61:648–665.
502	Georgian SE, Dupont S, Kurman M, Butler A, Strömberg SM, Larsson AI, Cordes EE. 2016b.
503	Biogeographic variability in the physiological response of the cold-water coral Lophelia
504	pertusa to ocean acidification. <i>Marine Ecology</i> 37:1345–1359. DOI: 10.1111/maec.12373.
505	Georgian SE, Shedd W, Cordes EE. 2014. High-resolution ecological niche modelling of the
506	cold-water coral Lophe pertusa in the Gulf of Mexico. Marine Ecology Progress Series
507	506:145–161. DOI: 10.3354/meps10816.
508	Gleckler PJ, Durack PJ, Stouffer RJ, Johnson GC, Forest CE. 2016. Industrial-era global ocean
509	heat uptake doubles in recent decades. <i>Nature Climate Change</i> 6:394–398. DOI:
510	10.1038/nclimate2915.
511	Gómez CE, Wickes L, Deegan D, Etnoyer PJ, Cordes EE. 2018. Growth and feeding of deep-sea
512	coral Lophelia pe a from the California margin under simulated ocean acidification
513	conditions. <i>PeerJ</i> 2018. DOI: 10.7717/peerj.5671.
514	Guinotte JM, Orr J, Cairns S, Freiwald A, Morgan L, George R. 2006. Will human-induced
515	changes in seawater chemistry alter the distribution of deep-sea scleractinian corals?
516	Frontiers in Ecology and the Environment 4:141–146.
517	Häussermann V, Försterra G. 2007. Extraordinary abundance of hydrocorals (Cnidaria,
518	Hydrozoa, Stylasteridae) in shallow water of the Patagonian fjord region. Polar Biology
519	30:487–492. DOI: 10.1007/s00300-006-0207-5.



520	Henry LA. 2011. A deep-sea coral 'gateway'in the northwestern Caribbean. <i>Palomares MLD</i> ,
521	Pauly D Too Precious to Drill: the Marine Biodiversity of Belize:120–124.
522	Hernández-Ávila I. 2014. Patterns of deep-water coral diversity in the bbean basin and
523	adjacent southern waters: An approach based on records from the R/V pushury
524	editions. PLoS ONE 9. DOI: 10.1371/journal.pone.0092834.
525	Huang W, Wang Y, Cai W. 2012. Assessment of sample storage techniques for total alkalinity
526	and dissolved inorganic carbon in seawater. Limnology and oceanography: Methods
527	10:711–717.
528	Lunden JJ, Georgian SE, Cordes EE. 2013. Aragonite saturation states at cold-water coral reefs
529	structured by Lopheli ertusain the northern Gulf of Mexico. Limnology and
530	Oceanography 58:354–362. DOI: 10.4319/lo.2013.58.1.0354.
531	Miller KJ, Gunasekera RM. 2017. A comparison of genetic connectivity in two deep sea corals
532	to examine whether seamounts are isolated islands or stepping stones for dispersal.
533	Scientific Reports 7:1–14. DOI: 10.1038/srep46103.
534	Miloslavich P, Díaz JM, Klein E, Alvarado JJ, Díaz C, Gobin J, Escobar-Briones E, Cruz-Motta
535	JJ, Weil E, Cortés J, Bastidas AC, Robertson R, Zapata F, Martín A, Castillo J, Kazandjian
536	A, Ortiz M. 2010. Marine biodiversity in the caribbean: Regional estimates and distribution
537	patterns. PLoS ONE 5. DOI: 10.1371/journal.pone.0011916.
538	Montes E, Muller-karger FE, Cianca A, Lomas MW, Lorenzoni L, Habtes S. 2016. Decadal
539	variability in the oxygen inventory of North Atlantic subtropical underwater captured by
540	sustained, long-term oceanographic time series observations. Global Biogeochemical Cycle.
541	30:460–478. DOI: 10.1002/2015GB005183.Received.
542	Morrison JM, Nowlin WD. 1982. General distribution of water masses within the eastern



543	Caribbean Sea during the winter of 1972 and fall of 1973. Journal of Geophysical
544	Research: Oceans 87:4207–4229.
545	OBIS. 2019. Ocean Biogeographic Information System. Intergovernmental Oceanographic
546	Commission of UNESCO.
547	Pérez FF, Fontela M, Garcia-Ibañez MI, Mercier H, Velo A, Lherminier P, Zunino P, de la Paz
548	M, Alonso-Pérez F, Guallart EF, Padin XA. 2018. Meridional overturning circulation
549	conveys fast acidification to the deep Atlantic Ocean. <i>Nature</i> . DOI: 10.1038/nature25493.
550	Quattrini AM, Demopoulos AWJ, Singer R, Roa-Varon A, Chaytor JD. 2017. Demersal fish
551	assemblages on seamounts and other rugged features in the northeastern Caribbean. Deep
552	Sea Research Part I: Oceanographic Research Papers. DOI: 10.1016/j.dsr.2017.03.009.
553	Reed JK, Weaver DC, Pomponi SA. 2006. Habitat and fauna of deep-water Lophelia pertusa
554	coral reefs off the southeastern US: Blake Plateau, Straits of Florida, and Gulf of Mexico.
555	Bulletin of Marine Science 78:343–375.
556	Robbins LL, Hansen ME, Kleypas JA, Meylan SC. 2010. CO2calc: A user-friendly seawater
557	carbon calculator for Windows, Mac OS X, and iOS (iPhone). US Geological Survey.
558	Roberts JM, Wheeler A, Freiwald A, Cairns SD. 2009. Cold-water corals: the biology and
559	geology of deep-sea coral habitats. Cambridge University Press.
560	Rogers AD. 1994. The biology of seamounts. In: Advances in marine biology. Elsevier, 305–
561	350.
562	Rogers AD. 2018. The Biology of Seamounts: 25 Years on. Advances in Marine Biology
563	79:137–224. DOI: 10.1016/BS.AMB.2018.06.001.
564	Santodomingo N, Reyes J, Gracia A, Martínez A, Ojeda G, García C. 2007. Azooxanthellate
565	Madracis coral communities off San Bernardo and Rosario Islands (Colombian Caribbean).

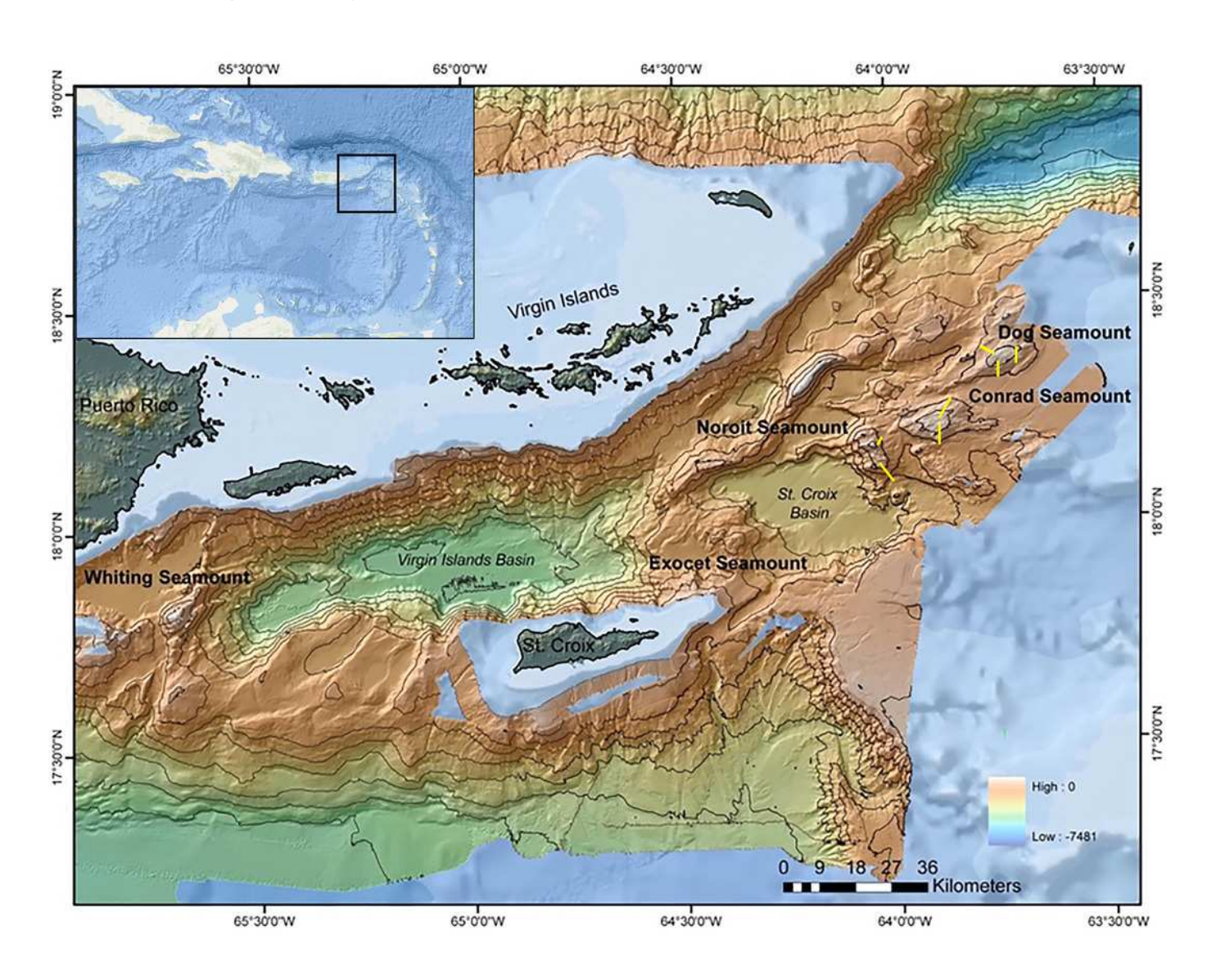




566	Bulletin of Marine Science 81:273–287.
567	Schroeder WW, Brooke SD, Olson JB, Phaneuf B, McDonough JJ, Etnoyer P. 2005. Occurrence
568	of deep-water Lophelia pertusa and Madressa oculata in the Gulf of Mexico. In: Cold-
569	water corals and ecosystems. Springer, 297–307.
570	Thresher RE, Tilbrook B, Fallon S, Wilson NC, Adkins J. 2011. Effects of chronic low carbonate
571	saturation levels on the distribution, growth and skeletal chemistry of deep-sea corals and
572	other seamount megabenthos. <i>Marine Ecology Progress Series</i> 442:87–99. DOI:
573	10.3354/meps09400.
574	Venn A, Tambutté E, Holcomb M, Allemand D, Tambutté S. 2011. Live tissue imaging shows
575	reef corals elevate pH under their calcifying tissue relative to seawater. <i>PLoS ONE</i> 6. DOI:
576	10.1371/journal.pone.0020013.
577	

Multibeam bathymetric map of the Anegada Passage seamounts.

The location of Dog, Conrad, and Noroît Seamounts is indicated in bold. Transect locations are overlaid in yellow segments.

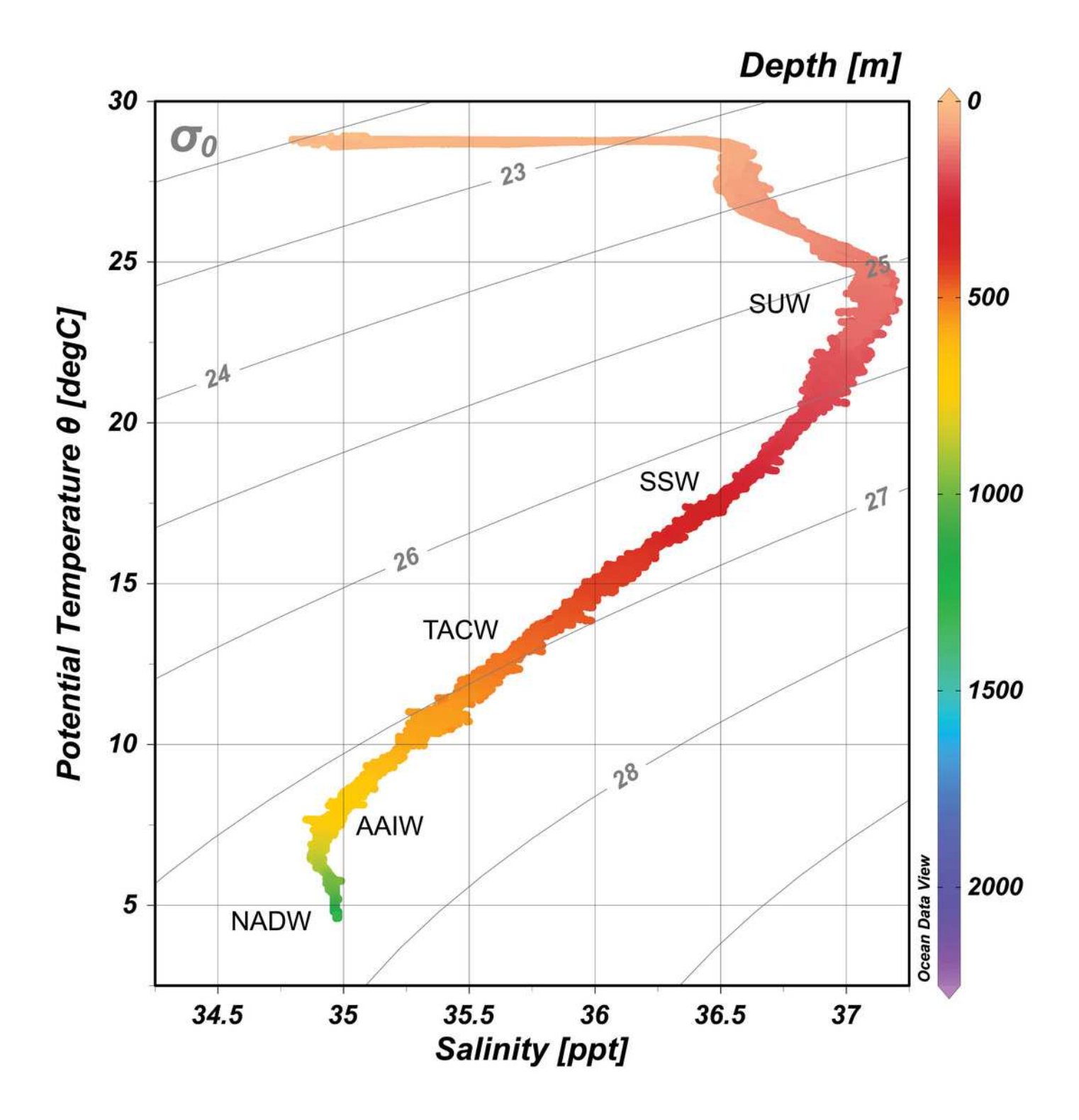




Temperature-Salinity plot for the Anegada Passage based on CTD water column profiles.

Water masses are overlaid and abbreviated by the following: SUW=Subtropical underwater, SSW=Sargasso Sea Water, TACW= Tropical Atlantic Central Water, AAIW=Antarctic Intermediate Water, and NADW=North Atlantic Deep Water.

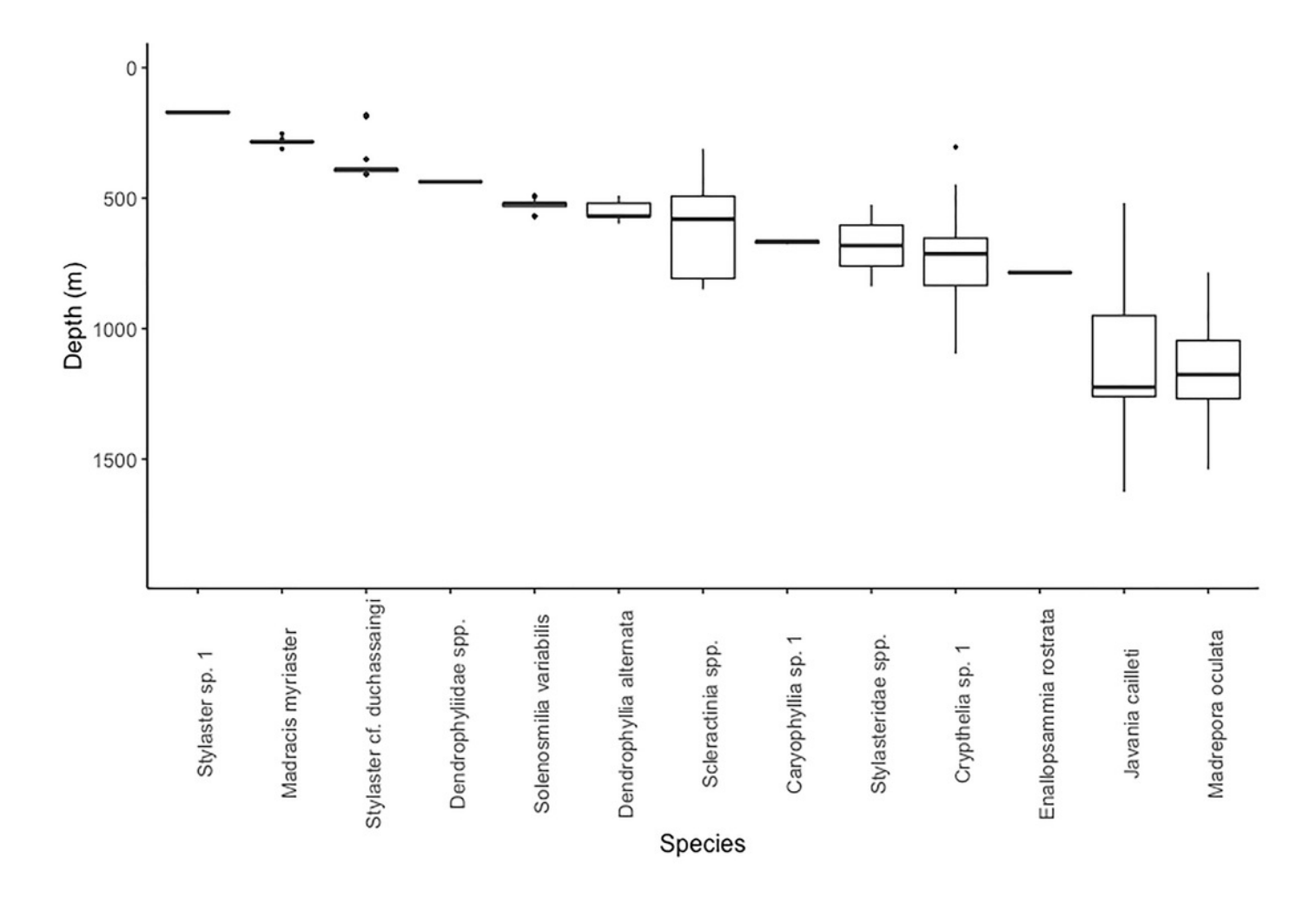






Boxplot of depth distribution for each of 13 species occurring on Dog, Conrad, and Noroît Seamounts.

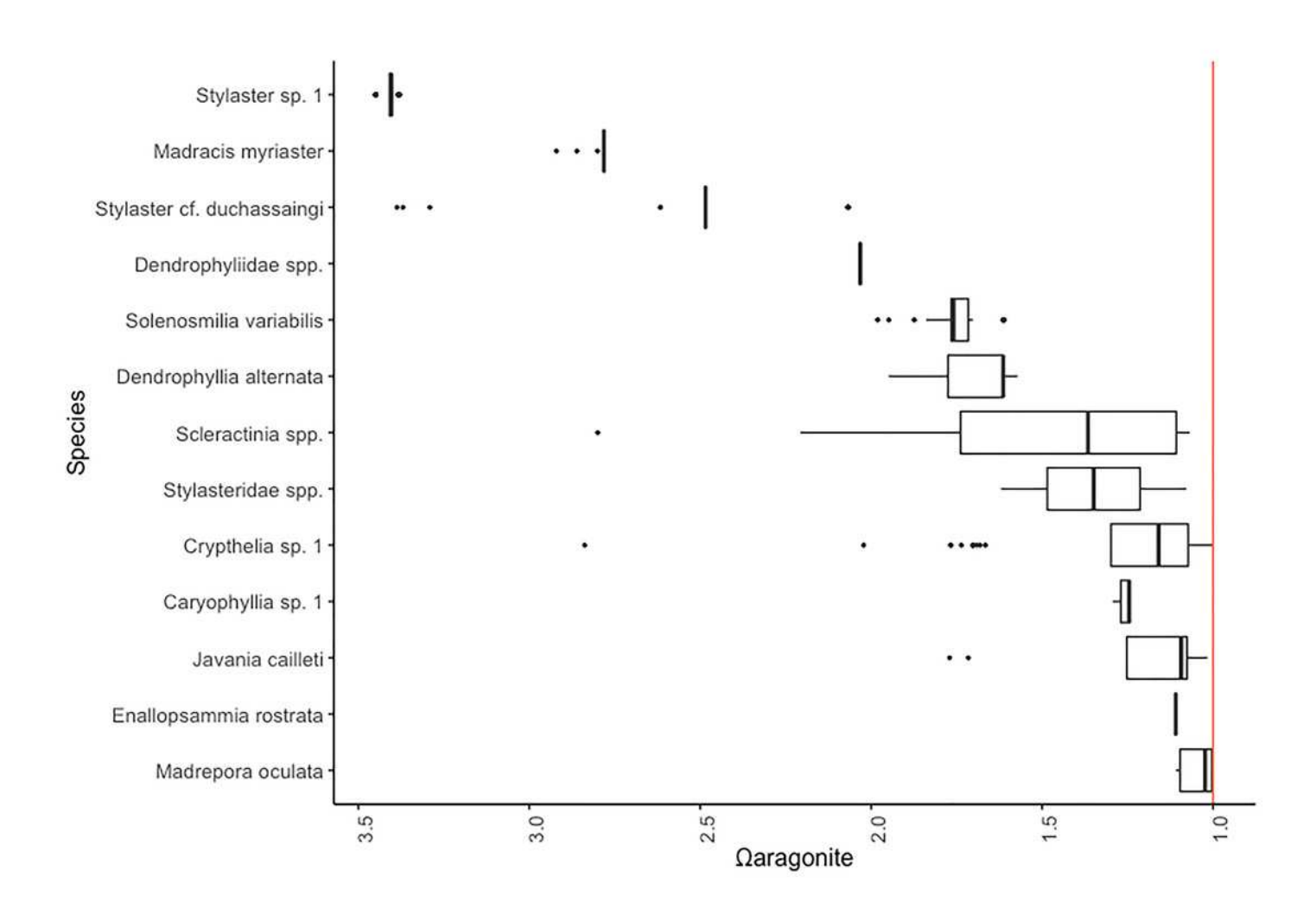
Species are arranged on the x-axis from highest to lowest median depth of occurrence.





Distribution of 13 morphospecies against predicted Ω_{Arag} values in the Anegada Passage.

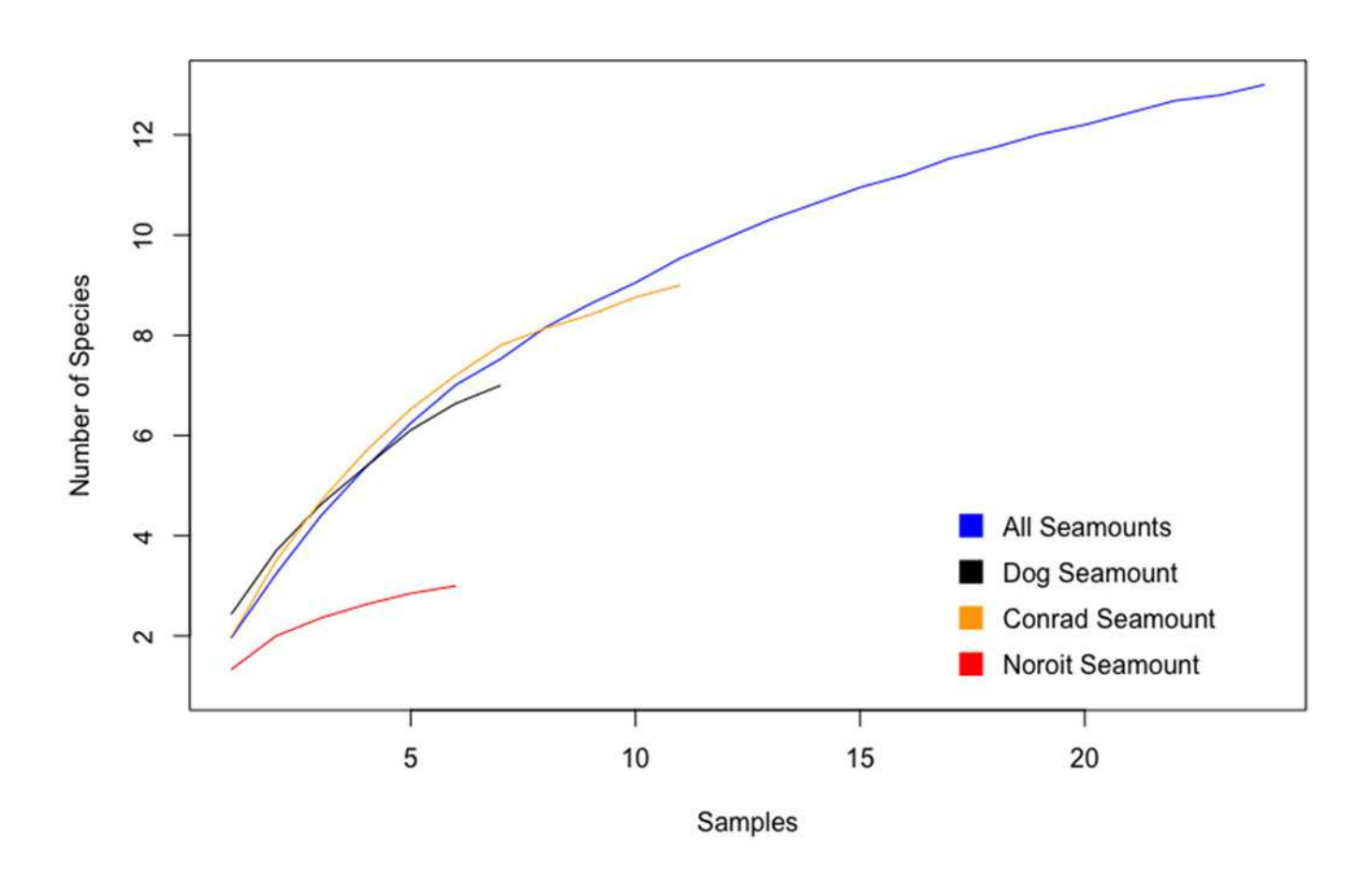
Species are arranged on the y-axis from highest to lowest median aragonite saturation occurrence. A solid red line indicates the saturation horizon where $\Omega_{Arag}=1$.





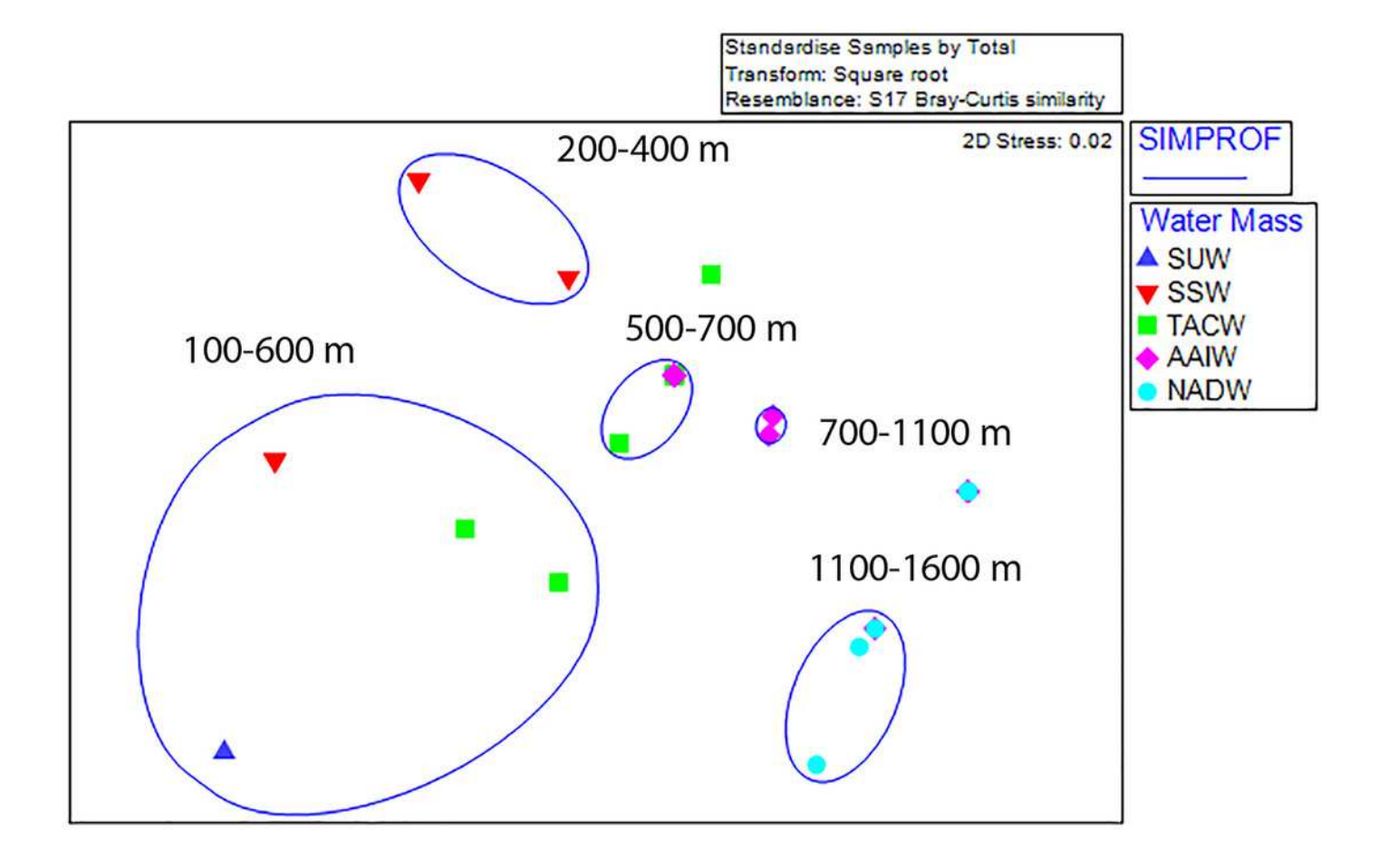
Species accumulation curves for the Anegada Passage seamounts.

Curves are separate for all transects on Dog Seamount, Conrad Seamount, Noroit Seamount, and all seamounts pooled.



Nonmetric multidimensional scaling analysis of fourth-root transformed coral assemblages by on Dog, Conrad, and Noroît Seamounts.

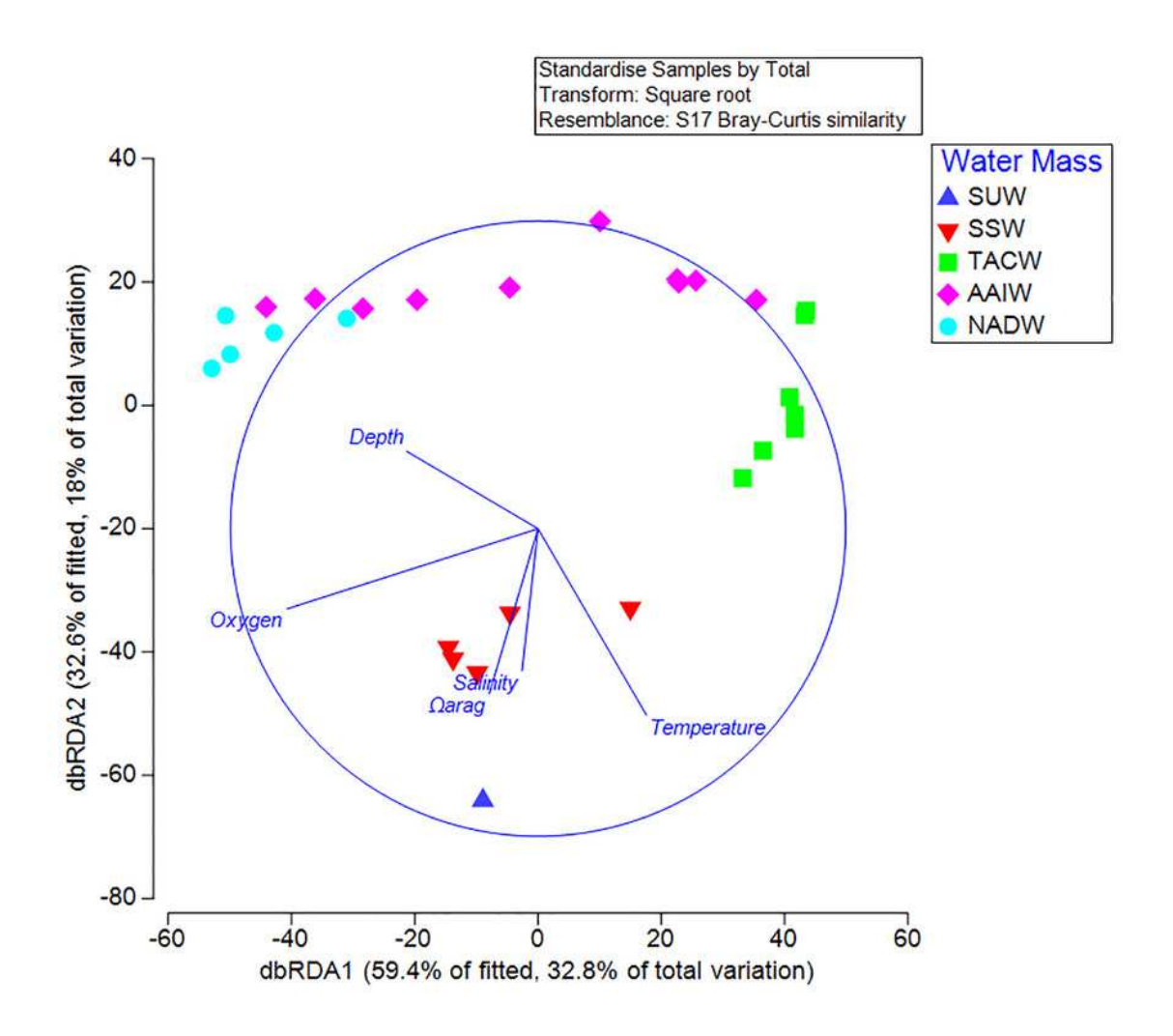
SIMPROF groups are overlaid around significant groupings at the 95% level or above. Depth ranges displayed within each statistical grouping are indicated in black text.





Distance-based linear model and redundancy analysis of coral assemblages and oceanographic variables.

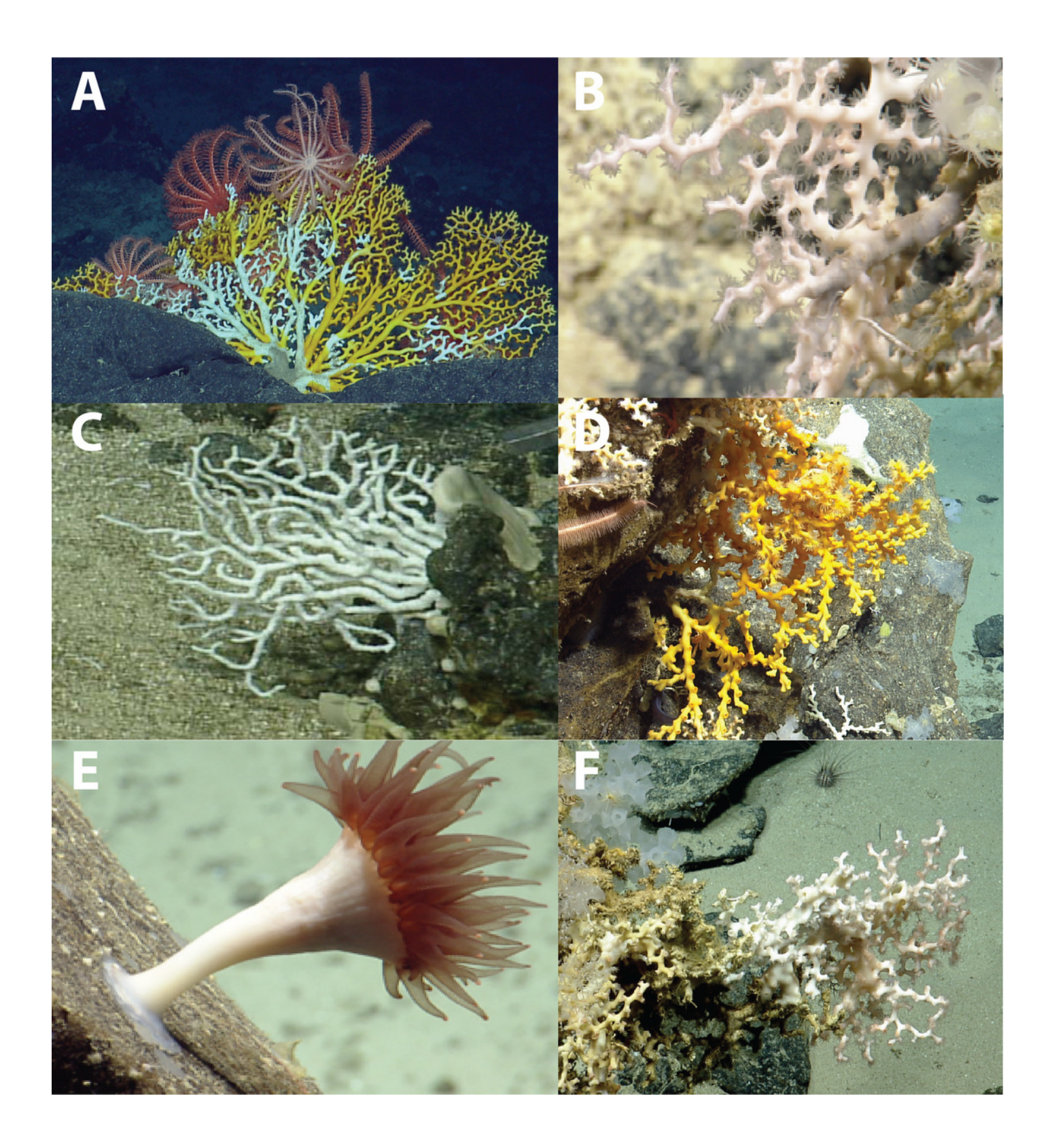
Sample points represent one 100 m depth assemblage. Axes shown are the results of a distance-based redundancy analysis with percent variation explained by the first and second axes.





Deep-water scleractinians from the Anegada Passage seamounts.

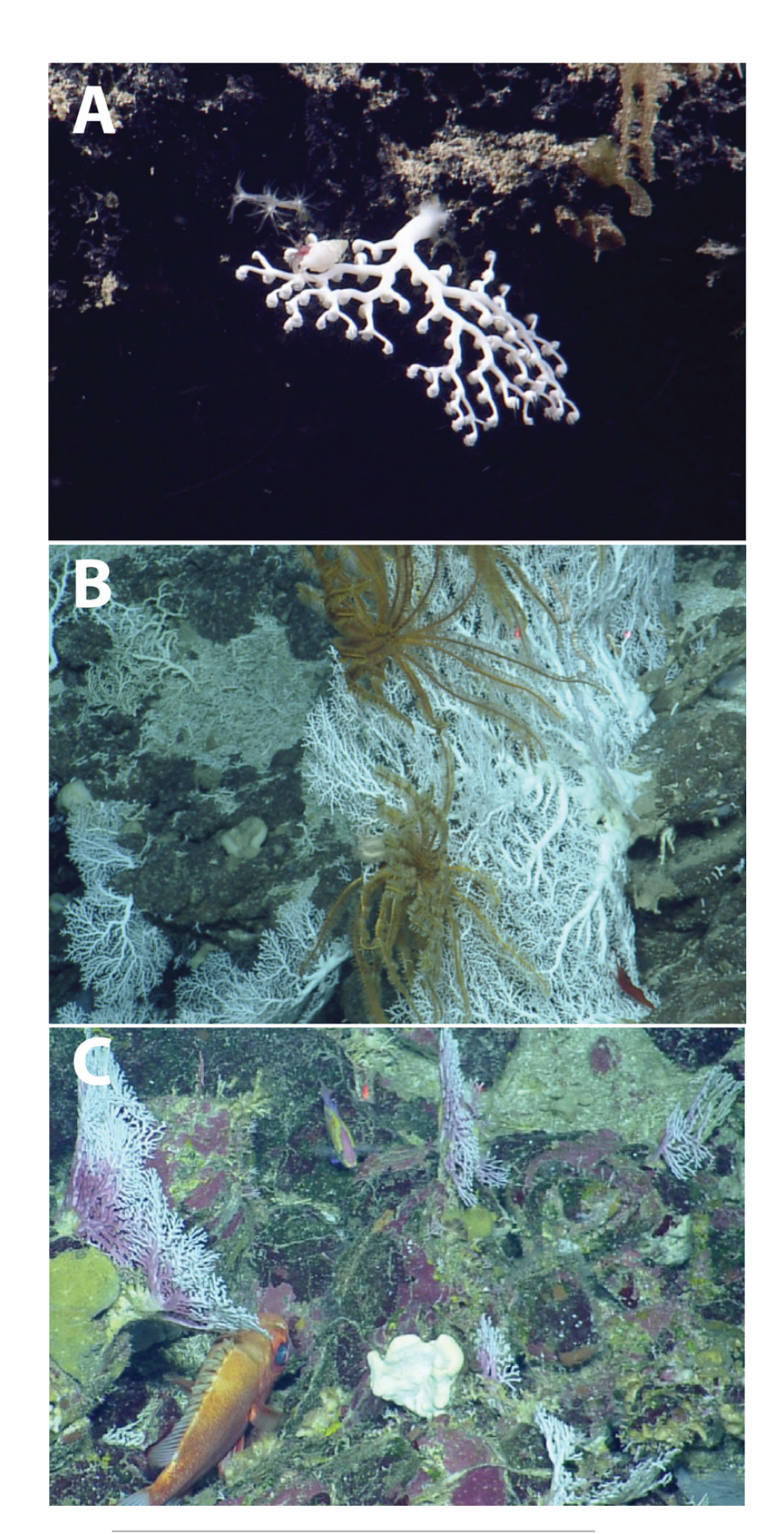
(A) Enallopsammia rostrata, (B) Madrepora oculata, (C) Madracis myriaster, (D) Dendrophyllia alternata, (E) Javania cailleti, (F) Solenosmilia variabilis.





Deep-water stylasterids from the Anegada Passage seamounts.

(A) Crypthelia sp. 1, (B) Stylaster cf. duchassaingi, (C) Stylaster sp. 1.



PeerJ reviewing PDF | (2018:04:27834:0:0:NEW 24 Jan 2020)



Table 1(on next page)

ROV dive transect details for 2014 surveys of the Anegada Passage seamount.

Included are start and end coordinates for each transect, time spent in visual contact with the seafloor, and number of water samples collected at depth over the dive interval.



- 1 Table 1: ROV dive transect details for 2014 surveys of the Anegada Passage seamounts.
- 2 Included are start and end coordinates for each transect, time spent in visual contact with the
- 3 seafloor, and number of water samples collected at depth over the dive interval.

Dive	Seam ount	Start Coordinates	End Coordinates	Depth Range (m)	Number of Niskin Bottle Samples	Total Bottom Time (hh:mm:ss)
H137 2	Dog	18°18.7385 N 63°46.0896 W	18°19.6177 N 63°46.1645 W	717-1035	6	7:56:00
H137	Dog	18°22.6480 N 63°46.1953 W	18°21.9711 N 63°45.9306 W	503-784	6	11:09:47
H137 4	Dog	18°20.4464 N 63°43.6091 W	18°21.9311 N 63°43.5024 W	276-601	5	9:58:00
H137 5	Conra d	18°10.5420 N 63°53.1020 W	18°13.0029 N 63°53.3459 W	162-876	5	31:40.43
H137 6	Conra d	18°16.4904 N 63°52.3364 W	18°14.2223 N 63°52.9767 W	344-1267	6	22:38:00
H137 7	Noroît	18° 05.4657 N 64° 00.1741 W	18° 07.0695 N 64° 01.1760 W	881-2157	6	17:10.38
H137 8	Noroît	18° 09.6969 N 64° 01.3606 W	18° 09.4122 N 64° 01.8888 W	949-1035	2	06:01:50



Table 2(on next page)

Summary of records and environmental variables for each taxon.

Ranges of values for abundance, depth, temperature, dissolved oxygen, model predicted Ω_{Arag} , and colony height are reported species by taxonomic grouping.

- 1 Table 2: Range of values of abundance, depth, temperature, dissolved oxygen, model predicted Ω_{Arag} , and colony height for each
- 2 reported species.

Class	Family	Species	Number of observations	Depth (m)	Temperature (°C)	Salinity (psu)	Dissolved oxygen (mg/L)	Predicated Ω_{arag}	Height (cm)
Hydrozoa	Stylasteridae	Stylaster sp. 1	65	166-174	22.1-22.5	37.00-37.05	7-7.12	3.38-3.45	
		Crypthelia sp. 1	49	304-1096	4.9-18.0	34.53-36.55	2.41-7.22	0.99-2.83	1-12
		Stylaster cf. duchassaingi	30	181-408	13.8-22.1	35.82-37.01	5.39-6.99	2.07-3.39	12-37
		Stylasteridae spp.	2	525-838	6.7-10.9	34.89-35.39	4.96-5.28	1.08-1.62	3-5
	Caryophylliidae	Solenosmilia variabilis	44	490-569	10.9-13.3	35.37-35.75	4.88-5.15	1.61-1.98	12-18
		Caryophyllia sp. 1	3	665-677	8.2-8.7	35.03-35.07	4.78-4.86	1.24-1.29	
	Oculinidae	Madrepora oculata	22	784-1540	4.3-6.9	34.53-34.97	5.22-8.23	1.00-1.10	10-125
	Pocilloporidae	Madracis myriaster	22	253-311	17.6-18.7	36.49-36.65	6.83-7.01	2.78-2.92	6-35
	Incertae familiae	Scleractinia spp. (solitary)	11	311-849	6.5-17.8	34.83-36.51	4.76-6.98	1.07-2.8	4-5
	Dendrophylliidae	Dendrophyllia alternata	5	490-598	10.7-13	35.33-35.71	4.84-5.13	1.57-1.95	16
		Enallopsammia rostrata	2	785	7.0	34.921	5.2	1.11	20-75
		Dendrophyliidae spp.	1	437	13.6	35.794	5.29	2.03	5
	Flabellidae	Javania cailleti	8	518-1626	4.2-12.0	34.557-35.54	4.96-8.34	1.02-1.77	4-7



Table 3(on next page)

Summary of measured values of $\Omega_{\mbox{\tiny Arag}}$ from water samples taken directly adjacent to corals.



1 Table 3: Measured values of Ω_{Arag} from water samples taken directly adjacent to corals.

Class	Family	Species	Number of adjacent water samples	Ωarag measured
	Stylasteridae	Stylaster sp. 1	0	N/A
		Crypthelia sp. 1	0	N/A
Hydrozoa		Stylaster cf. duchassaingi	0	N/A
		Stylasteridae spp.	0	N/A
	Caryophylliidae	Solenosmilia variabilis	1	1.63
		Caryophyllia sp. 1	1	1.24
	Oculinidae	Madrepora oculata	2	1.13-1.16
	Pocilloporidae	Madracis myriaster	1	2.7
	Incertae familiae	Scleractinia spp. (solitary)	0	N/A
Anthozoa		Dendrophyllia alternata	1	1.35
	Dendrophylliidae	Enallopsammia rostrata	1	1.21
		Dendrophyliidae spp.	1	1.82
	Flabellidae	Javania cailleti	1	1.16